

## Impurity-diffusion investigations in amorphous $\text{Ti}_{60}\text{Ni}_{40}$

S. K. Sharma,\* M.-P. Macht, and V. Naundorf

*Hahn-Meitner-Institut Berlin, Glienicker Strasse 100, 14109 Berlin, Germany*

(Received 23 August 1993)

Tracer-diffusion coefficients  $D$  of the impurities B, Be, Fe, and Si in the amorphous alloy  $\text{Ti}_{60}\text{Ni}_{40}$  have been measured in the temperature range 598–690 K using the technique of secondary-ion-mass spectrometry for concentration depth profiling. The temperature dependence of the measured diffusion coefficients in each case exhibited an Arrhenius behavior and yielded the values of the activation energy  $Q$  in units of eV as  $(2.05 \pm 0.14)$ ,  $(2.20 \pm 0.15)$ ,  $(2.33 \pm 0.14)$ , and  $(2.35 \pm 0.15)$  for the diffusion of B, Be, Fe, and Si, respectively. The corresponding values of the preexponential factor of the diffusion coefficient  $D_0$  in units of  $\text{m}^2\text{s}^{-1}$  were obtained as  $7.4 \times 10^{(-4.0 \pm 1.1)}$ ,  $1.7 \times 10^{(-3.0 \pm 1.2)}$ ,  $2.5 \times 10^{(-3.0 \pm 1.1)}$ , and  $5.8 \times 10^{(-4.0 \pm 1.8)}$ . The results show the size dependence of  $D$  in this alloy according to which the small boron atoms diffuse about 2 orders of magnitude faster than the big silicon atoms while the diffusivities of Be and Fe had intermediate values following the trend  $D_B > D_{\text{Be}} > D_{\text{Fe}} > D_{\text{Si}}$  which is opposite to that of atomic radii  $r$  of the diffusing species, i.e.,  $r_{\text{Si}} > r_{\text{Fe}} > r_{\text{Be}} > r_B$ . The present data have been compared with those available in other amorphous alloys and in crystalline  $\alpha$ -Zr and  $\alpha$ -Ti. The notable distinct differences in the diffusion behavior in the amorphous and the crystalline cases are highlighted. On the basis of an observed correlation between the activation energy  $Q$  and the prefactor  $D_0$  the possible diffusion mechanism in amorphous alloys is discussed.

### I. INTRODUCTION

Amorphous metallic alloys are metastable structures which undergo structural relaxation and crystallization on thermal annealing. These kinetic processes lead to significant changes in many of their structure-sensitive properties. A considerable rearrangement of atoms occurs during these processes and thus a knowledge of atomic transport mechanisms is highly desirable for understanding pre- and post-crystallization changes of their properties.<sup>1</sup> The discovery of amorphization by solid-state reaction<sup>2</sup> has further added to the importance of diffusion investigations in these materials. In addition to these, a comparative study of the diffusion behavior in amorphous and crystalline materials is important for establishing any distinct differences in the nature of atomic transport processes in these two structurally different atomic environments.

There are two broad categories of amorphous metallic alloys, namely, the metal-metalloid (M-Me) and the metal-metal (M-M) types. Despite the fact that a considerable amount of diffusion investigations have been carried out in these materials, there are only limited systematic investigations.<sup>3–6</sup> Such systematic investigations are necessary in view of the uncertainties associated with the structural state of these materials due to relaxation, and those associated with the measurement of small diffusion distances (typically of the order of a few nanometers) in them. Small diffusion lengths are, in fact, a consequence of the narrow permissible range of annealing temperatures and times during which the metastable material remains amorphous without undergoing any crystallization. Experimental techniques having comparable depth resolution such as ion-beam microsectioning combined with the measurement of the activity of ra-

diotracers, secondary ion mass spectrometry (SIMS), Auger electron spectrometry (AES), and Rutherford backscattering spectrometry (RBS) have thus mostly been employed for direct measurement of these small diffusion lengths.<sup>5,7,8</sup>

The status of diffusion research in amorphous metallic alloys has been reviewed in several articles<sup>7–9</sup> and a recent compilation of the available diffusion data has also appeared.<sup>10</sup> It is noted that fewer diffusion investigations have been reported in M-M-type amorphous alloys as compared to those in M-Me-type amorphous alloys. Some notable systematic diffusion studies carried out on M-Me-type amorphous alloys include those on  $\text{Fe}_{40}\text{Ni}_{40}\text{B}_{20}$ ,<sup>3,5</sup>  $\text{Pd}_{78}\text{Cu}_{16}\text{Si}_6$ ,<sup>6</sup> and on the binary Fe-B (Ref. 11) alloys. On the other hand, among the M-M-type amorphous alloys, Zr-based alloys, e.g., Zr-Ni,<sup>4,12</sup> Zr-Fe,<sup>13</sup> Zr-Co,<sup>14</sup> and the amorphous Ni-Nb (Ref. 15) have mostly been considered for diffusion investigations.

Ti-Ni constitutes an important alloy system among the Ti-based alloys wherein amorphous alloys over a wide composition range have been produced.<sup>16,17</sup> Some of the attractive features of these alloys are their good thermal stability, excellent mechanical properties, and low-mass density. Moreover, the ternary additions of B, Be, and Si to Ti-based alloys (e.g., Ti-Zr-Be, Ti-Ni-B, and Ti-Ni-Si) have been found to result not only in high strength amorphous alloys with drastically enhanced thermal stability, but also in their easy quenchability in amorphous forms.<sup>17,18</sup> The kinetics of structural relaxation and crystallization of amorphous Ti-Ni alloys has been investigated several times [e.g., Refs. 19 and 20]. In contrast to this, not much attention has been paid to the diffusion behavior of these and other Ti-containing M-M-type amorphous alloys. The reported direct measurement of diffusion rates in Ti-Ni alloys include the data pertaining

to the diffusion of Si in  $\text{Ti}_{60}\text{Ni}_{40}$  (Ref. 21) and the preliminary measurements<sup>22</sup> of diffusion of several other impurity atoms in this alloy as well as the diffusion of B in  $\text{Co}_{74}\text{Ti}_{26}$ .<sup>23</sup>

The present study was started not only with the motivation to increase the data base of reliable diffusion measurements in Ti-based amorphous alloys but also to test for these M-M-type alloys some correlations which have been observed already in other amorphous alloys.<sup>12</sup> There are correlations which show a systematic dependence of the diffusion coefficient  $D$  and of the activation energy  $Q$  of diffusion on the size of the diffusing impurity, and a relationship between the preexponential factor  $D_0$  and the activation energy  $Q$  of the respective diffusion coefficients. We believe that these correlations, if they exist universally, are highly significant for a proper understanding of the yet unknown diffusion mechanism in amorphous alloys.

The present study reports on a set of data pertaining to the diffusion of the impurity atoms B, Be, Fe, and the previously investigated Si (Ref. 21) in amorphous  $\text{Ti}_{60}\text{Ni}_{40}$ . These diffusing species possess an appreciable difference in their atomic sizes, and it is therefore expected that the diffusivities show a sufficiently large variation in order to make the test of the above-mentioned correlations meaningful.

## II. EXPERIMENT

The material used in this investigation was a melt-spun amorphous ribbon (11 mm wide, 30  $\mu\text{m}$  thick) of the alloy  $\text{Ti}_{60}\text{Ni}_{40}$  produced by the Vakuumschmelze, Hanau, FRG. A characterization of this material by x-ray diffraction (XRD) and transmission electron microscopy (TEM) showed that the wheel side of the ribbon (i.e., the nonshiny side, which was in direct contact with the cooling copper wheel during production) was completely amorphous, while the air side of the ribbon (i.e., the shiny side) contained some crystalline fraction in addition to the bulk amorphous phase due to the somewhat slower cooling rate. Therefore, the wheel side was used for diffusion measurements in the present investigation. Specimens, each measuring about 11 mm in length, were cut from the as-received ribbon of the alloy. The wheel side was mechanically polished first with 3  $\mu\text{m}$  and then with 1- $\mu\text{m}$  diamond abrasive to remove a layer of about 5  $\mu\text{m}$  thickness of the material. During this mechanical polishing much lubricant was used to minimize the specimen heating. The polished specimens were thermally relaxed at 620 K for 2 h in a high vacuum furnace (pressure  $< 10^{-4}$  Pa). An XRD check of the polished side of the relaxed specimens confirmed their amorphous nature. It should be noted that all the diffusion coefficients reported in the present study correspond to those in the relaxed state of the amorphous alloy.

Diffusion specimens were prepared in a UHV chamber under argon pressure of  $10^{-4}$  Pa without breaking the vacuum. In a first step the polished surface of the relaxed specimens was cleaned by argon-ion etching in order to remove residual contaminations. In a second step between about 0.2 and 2  $\mu\text{g}/\text{cm}^2$  of the diffusing species

were sputter deposited onto an area of 9 mm diameter of the cleaned surface. In a last step finally the thin tracer layer was covered by about 50 nm of the sputter-deposited  $\text{Ti}_{60}\text{Ni}_{40}$  base material in order to form an amorphous sandwich specimen with the thin impurity layer at a predefined position. The pure elemental targets of Be or Fe were employed for the sputter deposition of the tracer layers of Be or Fe, respectively. In order to evaluate the diffusivities of B, a tracer layer of FeNiB was sputter deposited from a compound target which consisted of the metallic glass  $\text{Fe}_{40}\text{Ni}_{40}\text{B}_{20}$ . It was realized that this procedure would permit the simultaneous evaluation of the diffusivities of both B and Fe from one and the same specimen. An independent check of the diffusivity values of Fe was made by comparing these values with the diffusion rates obtained from the specimens on which a tracer layer of pure iron was sputter deposited. It is assumed that the effect of any interaction between the constituents of the FeNiB tracer layer in their dilute concentration on the diffusion rates of the respective tracers is quite insignificant.

The specimens were diffusion annealed between 602 and 690 K at selected temperatures and times in a high vacuum (pressure  $< 10^{-4}$  Pa) furnace having a temperature accuracy of  $\pm 1.5$  K. In the case of the earlier investigated Si,<sup>21</sup> the temperature range was 598–690 K. The annealing temperatures and the time periods are mentioned in Tables I–III for the different impurities. XRD measurements were taken from both sides of the annealed specimens. A significant crystallization was noticed at the air side. However, our measurements were made on the wheel side which was found to be completely amorphous at least up to a depth of several microns as probed by the XRD. Considering the small diffusion lengths the thickness of the amorphous zone extending from the wheel side was large enough to yield diffusion coefficients in the amorphous phase of the alloy. Some of the diffusion-annealed specimens were also checked by TEM and the wheel side was found to be amorphous.

The concentration depth profiles of the impurity layers were obtained by using the technique of secondary ion mass spectrometry. A primary beam of 4-keV  $\text{O}_2^+$  ions was used for sectioning. It was raster scanned to produce a flat-bottomed sputter crater of 1 mm  $\times$  1 mm. Concentration depth profiles of the impurities Be, B, or Fe were

TABLE I. Diffusion coefficients of Be in amorphous  $\text{Ti}_{60}\text{Ni}_{40}$ .

Specimen no.	Anneal temp. $T$ (K)	Anneal time $t$ ( $10^3$ s)	$D$ ( $10^{-20}$ $\text{m}^2 \text{s}^{-1}$ )
1	604	502.2	$8.5 \times 10^{-2}$
2	612	320.7	$1.3 \times 10^{-1}$
3	619	239.4	$1.9 \times 10^{-1}$
4	632	82.08	$4.3 \times 10^{-1}$
5	633	73.5	$5.9 \times 10^{-1}$
6	642	32.7	$7.5 \times 10^{-1}$
7	653	16.5	2.0
8	666	7.38	3.7
9	667	7.2	4.2
10	690	2.4	15.0

TABLE II. Diffusion coefficients of Fe in amorphous  $\text{Ti}_{60}\text{Ni}_{40}$ .

Specimen no.	Anneal temp. $T$ (K)	Anneal time $t$ ( $10^3$ s)	$D$ ( $10^{-20}$ $\text{m}^2 \text{s}^{-1}$ )
1	602	530.7	$8.3 \times 10^{-3}$
2	611	404.7	$1.4 \times 10^{-2}$
3	619	243.9	$2.5 \times 10^{-2}$
4	632	82.08	$6.4 \times 10^{-2}$
5	653	16.5	$2.6 \times 10^{-1}$
6	665	7.50	$5.6 \times 10^{-1}$
7	676	3.42	1.1
8	688	2.4	2.0

obtained under identical experimental conditions from the same specimen before and after the diffusion annealing. In this way a diffusional broadening of less than 5 nm could be resolved. SIMS measurements provide no absolute depth scale, as the relative concentration versus time-integrated ion current is monitored. Thus, for depth calibration of the concentration profiles the depth of the sputter craters after the completion of the SIMS analysis was measured directly on some specimens by a surface profilometer (DEKTAK, Veeco) to determine the sputtering rate. For the metallic glass  $\text{Ti}_{60}\text{Ni}_{40}$  used in the present investigation, this rate was determined to be 0.05 nm/ $\mu\text{As}$  (which corresponds to about 0.015 nm/s for the ion current of about 0.3  $\mu\text{A}$  used in the present experiments). The accuracy of this depth calibration was  $\pm 15$ – $25\%$  and was limited mainly by the waviness present on the polished specimen surfaces.

### III. DATA ANALYSIS AND RESULTS

The specimen geometry employed for diffusion measurements was that of a thin layer sandwiched in the amorphous matrix. Therefore, the diffusion coefficients were evaluated by using the thin-film solution<sup>24</sup> of the diffusion equation, namely,

$$C(x, t) = A(\pi Dt)^{-1/2} \exp(-\Delta x^2/4Dt), \quad (1)$$

TABLE III. Diffusion coefficients of boron ( $D_B$ ) and iron ( $D_{\text{Fe}}$ ) obtained from the simultaneous diffusion of Fe, Ni, and B in amorphous  $\text{Ti}_{60}\text{Ni}_{40}$ .

Specimen no.	Anneal temp. $T$ (K)	Anneal time $t$ ( $10^3$ s)	$D_B$ ( $10^{-20}$ $\text{m}^2 \text{s}^{-1}$ )	$D_{\text{Fe}}$ ( $10^{-20}$ $\text{m}^2 \text{s}^{-1}$ )
1	604	502.2	$5.2 \times 10^{-1}$	$5.0 \times 10^{-3}$
2	612	320.7	$9.5 \times 10^{-1}$	$1.8 \times 10^{-2}$
3	619	239.4	1.3	$2.8 \times 10^{-2}$
4	633	73.5	3.7	$3.8 \times 10^{-2}$
5	637	56.1	4.2	$7.0 \times 10^{-2}$
6	642	32.7	5.3	$1.2 \times 10^{-1}$
7	653	16.5	11.0	$2.5 \times 10^{-1}$
8	658	11.52	15.0	$4.1 \times 10^{-1}$
9	667	7.2	23.0	$4.2 \times 10^{-1}$
10	677	3.3	35.0	$9.7 \times 10^{-1}$
11	690	2.4	73.0	2.2

where  $C(x, t)$  is the impurity concentration,  $\Delta x = (x - x_0)$  is the distance measured from the thin layer position  $x_0$ ,  $t$  is the diffusion time,  $D$  is the diffusion coefficient, and  $A$  is the total amount of the tracer. The concentration depth profiles were analyzed on the basis of Eq. (1) assuming that the concentration  $C$  is proportional to the measured SIMS intensity of the impurity. The logarithm of the SIMS intensity of the diffusing tracer was plotted against the square of the depth  $\Delta x^2$  to yield the diffusion penetration plots. The diffusion coefficients of the tracer impurity atoms were determined from the mean slopes of the straight Gaussian fits to the penetration plots of  $\ln C$  versus  $\Delta x^2$ . If  $s_0$  and  $s$  are the mean slopes obtained from the penetration plots before and after the diffusion annealing for a time  $t$ , respectively, then the diffusion coefficient  $D$  is calculated from the relation

$$D = (1/s - 1/s_0)/4t. \quad (2)$$

Figures 1 and 2 represent the typical penetration plots and the Gaussian fits for Be and Fe diffusion in amorphous  $\text{Ti}_{60}\text{Ni}_{40}$ , respectively. The corresponding plots for the diffusion of B and Fe obtained from the alloy layer of FeNiB are shown in Figs. 3(a) and 3(b), respectively. All the data were background corrected before obtaining these plots. Two features are worth noticing from these plots: (i) the curves bend up in the vicinity of the concentration maximum, i.e., at  $\Delta x = 0$  [cf. Figs. 1 and 3(a)] and a slight overall curvature is visible which is most pronounced in the plots for the nonannealed specimens (cf. Fig. 2). The first feature pertaining to the enhanced intensity in the vicinity of the concentration maximum is

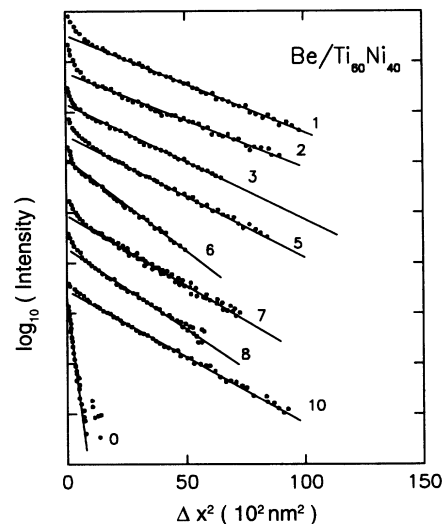


FIG. 1. Typical Gaussian penetration plots corresponding to the diffusion of Be in amorphous  $\text{Ti}_{60}\text{Ni}_{40}$ . The logarithm of Be intensity as measured by SIMS is given after background correction as a function of  $\Delta x^2 = (x - x_0)^2$ , where  $x_0$  is the position of the maximum in the concentration profile. The specimen number indicated on the plot refers to the annealing conditions which are given in Table I. The lower curve denoted by "0" is an example of the nonannealed state.

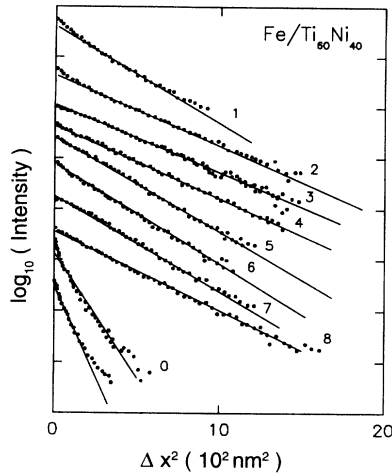


FIG. 2. Typical Gaussian penetration plots corresponding to the diffusion of Fe in amorphous  $\text{Ti}_{60}\text{Ni}_{40}$ . The measurements were carried out using pure Fe. The specimen number indicated on the plot refers to the annealing conditions which are given in Table II. The curves denoted by "0" correspond to the nonannealed state.

attributed to an enhancement in the ionization probability during SIMS analysis. This enhancement arises probably due to contamination with the residual gas atmosphere (mainly oxygen, nitrogen, and water vapors in the pressure range of  $< 10^{-6}$  Pa) during specimen preparation in the UHV chamber.<sup>25</sup> However, such contamination has no effect on the diffusion behavior of the tracer impurity atom outside the contaminated region. The data evaluation was thus restricted to the region lying well outside the contaminated zone. The other noteworthy feature relating to the slight curvature in some of the Gaussian plots due to atomic mixing effects during the sputter sectioning process which are known to produce exponentially decaying concentration profiles.<sup>26</sup>

The slopes used for calculating  $D$  according to Eq. (2) were obtained from the least-mean-squares fits to the penetration plots shown in Figs. 1–3. Limits for these fits were chosen in such a way that the minimum intensity considered was a factor of 2 higher than the observed background intensity level, and the maximum intensity was lying well outside the contaminated region near the concentration maximum at  $\Delta x = 0$ . As a result of the subtraction procedure employed in Eq. (2) for calculating  $D$  from the slopes of the penetration plots before and after annealing, the influence of the above-mentioned atomic mixing effects on the evaluation of diffusion coefficients are considerably reduced. The  $D$  values for the diffusion of Be, B, and Fe are summarized in Tables I–III. The temperature dependence of these diffusion coefficients is shown in the form of an Arrhenius plot in Fig. 4. The errors of the  $D$  values reported here resulted mainly from the error in the depth calibration and amounted to 30–50%. They were estimated for different series of measurements separately.

It is observed from Fig. 4 that the temperature dependence of the diffusivity of the impurity atoms B, Be, Fe

and Si in the amorphous alloy  $\text{Ti}_{60}\text{Ni}_{40}$  is Arrhenius in nature over the whole investigated temperature range from 598 to 690 K. The values of the diffusion parameters, viz., the activation energy  $Q$  and the prefactor  $D_0$  as obtained from fits of  $D = D_0 \exp(-Q/k_B T)$  to the data in Fig. 4, are given in Table IV.

As described above, the diffusion coefficients of Fe were evaluated from the compound layer of FeNiB which yielded the diffusivity values of both B and Fe in one and the same specimen. In order to check the correctness of the diffusivity values obtained by this procedure, the diffusion rates of Fe were also measured in those specimens on which a layer of pure Fe was sputter deposited. It is seen from Fig. 4 and Table IV that both these pro-

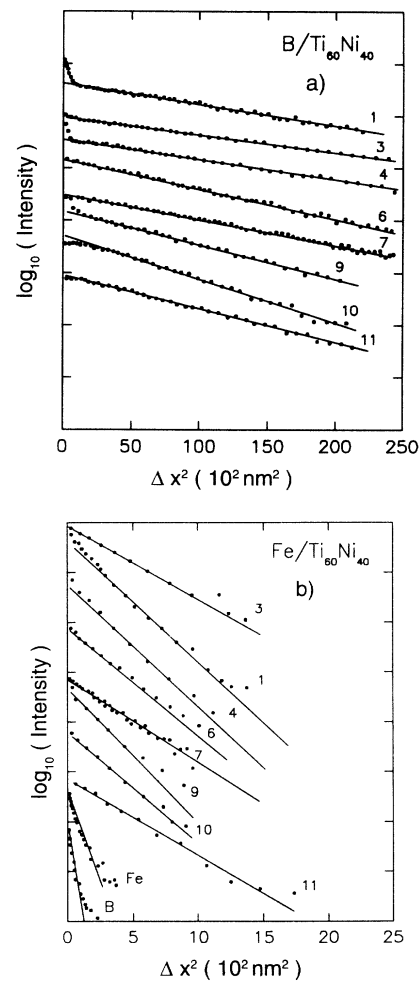


FIG. 3. (a) Typical Gaussian penetration plots corresponding to the diffusion of B in amorphous  $\text{Ti}_{60}\text{Ni}_{40}$ . The specimen number indicated on the plot refer to the annealing conditions given in Table III. (b) Typical Gaussian penetration plots corresponding to the diffusion of Fe in amorphous  $\text{Ti}_{60}\text{Ni}_{40}$ . The lower curves denoted by B and Fe are from the nonannealed specimens containing B and Fe, respectively. A layer of the FeNiB alloy sputter deposited from the amorphous target  $\text{Fe}_{40}\text{Ni}_{40}\text{B}_{20}$  was used in both of these measurements. The specimen numbers indicated on the plot refer to the annealing conditions given in Table III.

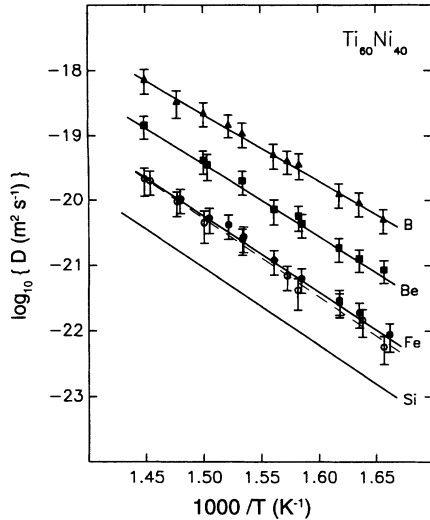


FIG. 4. The temperature dependence of the diffusion coefficients of B, Be, Fe, and Si in amorphous  $\text{Ti}_{60}\text{Ni}_{40}$  in the Arrhenius plot. Open symbols indicate diffusion coefficients of Fe obtained from the simultaneous diffusion of Fe, Ni, and B. Si data are taken from Ref. 21.

cedures yielded the same diffusivities within experimental uncertainty. It is thus concluded that B has no significant influence on the diffusivity of Fe in the present investigation.

#### IV. DISCUSSION

##### A. Comparison with data in other amorphous alloys and in crystalline $\alpha$ -Ti and $\alpha$ -Zr

Except the data of this study, no other direct measurements of diffusion coefficients in an amorphous Ti-Ni alloy have been reported. The preliminary results of this systematic investigation have been reported previously.<sup>22</sup> However, two indirect estimates of diffusion coefficients in compositionally different amorphous Ti-Ni alloys at some specific temperatures only have been made. A diffusion coefficient of about  $10^{-19} \text{ m}^2 \text{ s}^{-1}$  at 750 K has been reported in an investigation dealing with the crystallization of amorphous  $\text{Ti}_{40}\text{Ni}_{60}$ ,<sup>27</sup> while a diffusion coefficient of about  $10^{-22} \text{ m}^2 \text{ s}^{-1}$  at a much lower temperature of 523 K has been estimated in an investigation on solid-state amorphization of a Ti/Ni multilayer specimen.<sup>28</sup> The diffusion coefficients estimated in these inves-

tigations may be considered to represent interdiffusion coefficients in the respective binary Ti-Ni alloy. A comparison of these diffusion data may be attempted with the diffusion rates of Fe from the present investigation. The diffusion coefficient derived from the solid-state amorphization<sup>28</sup> is higher than the diffusion coefficient of Fe by about 3 orders of magnitude ( $D_{\text{Fe}} = 8.9 \times 10^{-26} \text{ m}^2 \text{ s}^{-1}$  at 523 K). This difference is quite noteworthy because it resembles a respective difference between the diffusivities of Ni and Fe in the related amorphous alloy  $\text{Zr}_{50}\text{Ni}_{50}$  (Ref. 4) and is in agreement with the assumption that the rate of solid-state amorphization of TiNi is limited by the diffusion of Ni in the amorphous material. On the other hand, the diffusivity obtained from the crystallization of  $\text{Ti}_{40}\text{Ni}_{60}$  compares fairly well with our measurements in which, at 750 K, a diffusion coefficient of  $D_{\text{Fe}} = 5.6 \times 10^{-19} \text{ m}^2 \text{ s}^{-1}$  is obtained. This may indicate an additional rate limiting process which could be related to the complicated morphology of crystalline TiNi and  $\text{TiNi}_3$  phases observed in this material.<sup>27</sup> In regard to impurity diffusion in amorphous alloys, it is worth mentioning that a strong compositional dependence for the diffusion of the impurity Cu in the M-M-type amorphous alloy Zr-Ni has earlier been reported.<sup>4</sup>

We shall compare in the following the data obtained in amorphous  $\text{Ti}_{60}\text{Ni}_{40}$  with those available for the diffusion of the same or similar-sized impurity atoms in other amorphous alloys. The diffusion data of all the species investigated here, namely, the B, Be, Fe, and Si have also been measured in the M-Me glass  $\text{Fe}_{40}\text{Ni}_{40}\text{B}_{20}$ .<sup>5,29,30</sup> The data for Be, Fe, and Si in  $\text{Fe}_{40}\text{Ni}_{40}\text{B}_{20}$  along with those in amorphous  $\text{Ti}_{60}\text{Ni}_{40}$  have been plotted in Fig. 5 in the form of normalized Arrhenius plots for  $D$ , i.e.,  $\ln D$  versus  $T_x/T$ , where  $T_x$  is the alloy crystallization temperature.

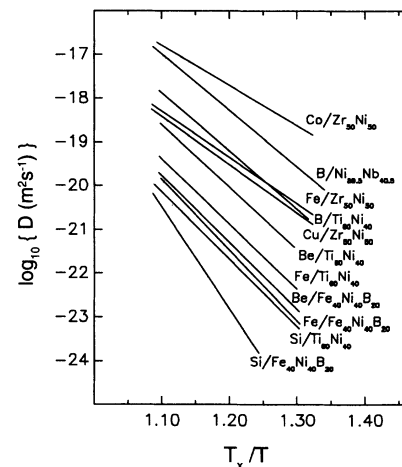


FIG. 5. The normalized Arrhenius plots of the diffusivity of various diffusants in the M-Me-type  $\text{Fe}_{40}\text{Ni}_{40}\text{B}_{20}$  and the M-M-type  $\text{Ti}_{60}\text{Ni}_{40}$ ,  $\text{Zr}_{50}\text{Ni}_{50}$ , and  $\text{Ni}_{59.5}\text{Nb}_{40.5}$  amorphous alloys. The values of the diffusion data for plotting these lines have been taken from the literature: Be, Si in  $\text{Fe}_{40}\text{Ni}_{40}\text{B}_{20}$  (Ref. 5); Fe in  $\text{Fe}_{40}\text{Ni}_{40}\text{B}_{20}$  (Ref. 30); Cu, Fe, Co in  $\text{Zr}_{50}\text{Ni}_{50}$  (Ref. 4); B in  $\text{Ni}_{59.5}\text{Nb}_{40.5}$  (Ref. 15); B, Be, Fe, and Si in  $\text{Ti}_{60}\text{Ni}_{40}$  (see Table IV).

TABLE IV. Diffusion parameters in amorphous  $\text{Ti}_{60}\text{Ni}_{40}$ .

Impurity at. radius (nm)	$D$ (650 K) ( $10^{-20} \text{ m}^2 \text{ s}^{-1}$ )	$Q$ (eV)	$D$ ( $10^{-3} \text{ m}^2 \text{ s}^{-1}$ )
B <sup>b</sup>	0.098	$2.05 \pm 0.14$	$7.4 \times 10^{(-1 \pm 1.1)}$
Be	0.112	$2.20 \pm 0.15$	$1.7 \times 10^{(\pm 1.2)}$
Fe <sup>a</sup>	0.126	$2.33 \pm 0.14$	$2.5 \times 10^{(\pm 1.1)}$
Fe <sup>b</sup>	0.126	$2.39 \pm 0.14$	$6.8 \times 10^{(\pm 1.1)}$
Si	0.132	$2.35 \pm 0.15$	$5.8 \times 10^{(-1 \pm 1.8)}$

<sup>a</sup>Using a pure Fe layer.

<sup>b</sup>Using an alloy layer of  $\text{Fe}_{40}\text{Ni}_{40}\text{B}_{20}$ .

The data for B diffusion in  $\text{Fe}_{40}\text{Ni}_{40}\text{B}_{20}$  (Ref. 29) have not been included in this figure in view of their non-Arrhenius nature. Such comparison of diffusion data in amorphous alloys on normalized Arrhenius plots has earlier been carried out<sup>5,7</sup> and these, in fact, are analogous to comparing data on  $\ln D$  versus  $T_m/T$  plots in crystalline materials ( $T_m$  is the melting temperature). It is observed from an intercomparison of normalized Arrhenius plots in Fig. 5 that the diffusivity of the same species at a given value of  $T_x/T$  is higher in  $\text{Ti}_{60}\text{Ni}_{40}$  than in  $\text{Fe}_{40}\text{Ni}_{40}\text{B}_{20}$ . This is consistent with the earlier observations<sup>7,31</sup> made from such normalized plots that the diffusion coefficient of a given species at the same value of the normalized fraction  $T_x/T$  is generally higher in an M-M-type than in an M-Me-type amorphous alloy. It is suggested that the energy barrier for the same migrating species is generally smaller in M-M-type than in M-Me-type amorphous alloys. This, in turn, would mean a more open structure for an M-M-type amorphous alloy in comparison to that for an M-Me-type one. As is known, there are basic structural differences between these two types of amorphous alloys. In particular, the metalloids in M-Me-type alloys are prevented from making any direct hard-sphere contact while the constituent metal atoms in M-M-type amorphous alloys prefer a more random distribution.<sup>32</sup> It appears that the structure of M-Me amorphous alloys, in which the metalloids are much smaller in size than the metallic constituents, is closer to a dense random packing than the structure of M-M-type amorphous alloys, where the size difference of the constituent metal atoms is not so large.<sup>32-34</sup> We note that in a recent investigation<sup>5</sup> diffusivity differences observed in the binary Fe-B and the ternary  $\text{Fe}_{40}\text{Ni}_{40}\text{B}_{20}$  have been correlated with the known structural differences of these amorphous alloys.

As regards the diffusion of B, Be, Fe, and Si in other M-M-type amorphous alloys, the data for the diffusion of B in  $\text{Co}_{76}\text{Ti}_{24}$  (Ref. 23) and  $\text{Ni}_{59.5}\text{Nb}_{40.5}$  (Ref. 15) and for the diffusion of Fe in  $\text{Zr}_{50}\text{Ni}_{50}$  (Ref. 4) have been reported. There are no data available for the diffusion of Be and Si in any other M-M amorphous alloys except those obtained in amorphous  $\text{Ti}_{60}\text{Ni}_{40}$  in the present study. Agreement is observed between the B diffusivity at 650 K in amorphous  $\text{Ti}_{60}\text{Ni}_{40}$  and  $\text{Co}_{74}\text{Ti}_{26}$  (Ref. 23) although in the latter alloy  $Q = 1.63$  eV and  $D_0 = 1.77 \times 10^{-7} \text{ m}^2 \text{ s}^{-1}$  are observed which are both smaller than the respective values in  $\text{Ti}_{60}\text{Ni}_{40}$  (cf. Table IV). The B data in  $\text{Co}_{74}\text{Ti}_{26}$  have not been plotted in Fig. 5 as the crystallization temperature of this alloy was not available. On the other hand, the B diffusion in  $\text{Ti}_{60}\text{Ni}_{40}$  is about 2-3 orders of magnitude faster than in  $\text{Ni}_{59.5}\text{Nb}_{40.5}$  when compared at the same temperature (say 650 K) while the Fe diffusion in  $\text{Ti}_{60}\text{Ni}_{40}$  is about 2 orders of magnitude slower than in  $\text{Zr}_{50}\text{Ni}_{50}$ . The much slower diffusion of B in  $\text{Ni}_{59.5}\text{Nb}_{40.5}$  could be attributed to the higher thermal stability of this alloy as is also revealed by its significantly higher crystallization temperature  $T_x$  [ $T_x = 953$  K for  $\text{Ni}_{59.5}\text{Nb}_{40.5}$  (Ref. 15) as compared to  $T_x = 770$  K for  $\text{Ti}_{60}\text{Ni}_{40}$  (Ref. 16)]. This assumption is supported by the presentation of the B diffusion data in Fig. 5 which shows that the values for the two alloys lie much closer together if they are compared at the same normalized temperature  $T/T_x$ .

The trend of an even lower B diffusivity in  $\text{Ti}_{60}\text{Ni}_{40}$  than in  $\text{Ni}_{59.5}\text{Nb}_{40.5}$  visible in this type of normalized plot might be traced back to a respective difference of the pre-factors  $D_0$  of the diffusion coefficients. As the crystallization temperatures of  $\text{Ti}_{60}\text{Ni}_{40}$  and  $\text{Zr}_{50}\text{Ni}_{50}$  do not differ considerably from each other [ $T_x = 750$  K for  $\text{Zr}_{50}\text{Ni}_{50}$  (Ref. 35)], the faster diffusion of Fe in  $\text{Zr}_{50}\text{Ni}_{50}$  than in  $\text{Ti}_{60}\text{Ni}_{40}$  is quite noteworthy (cf. Fig. 5).

In addition to the diffusion data of Fe, those of the similar-sized impurity atoms Cu and Co in  $\text{Zr}_{50}\text{Ni}_{50}$  have also been reported<sup>4</sup> and are plotted in Fig. 5. It is seen from this figure that Fe, Cu, and Co diffuse much faster in  $\text{Zr}_{50}\text{Ni}_{50}$  than the much smaller Be atoms in amorphous  $\text{Ti}_{60}\text{Ni}_{40}$ . This is an interesting observation and is perhaps related to the properties of the different matrices containing either Ti or Zr. In this regard, the diffusivity trends in crystalline  $\alpha$ -Ti and  $\alpha$ -Zr (Refs. 36 and 37) will be worth examining. In the case of crystalline  $\alpha$ -Ti and  $\alpha$ -Zr, the diffusivity values show the trend  $D_{\text{Co}}$  (in  $\alpha$ -Zr)  $>$   $D_{\text{Cu}}$  (in  $\alpha$ -Zr)  $>$   $D_{\text{Fe}}$  (in  $\alpha$ -Zr)  $>$   $D_{\text{Be}}$  (in  $\alpha$ -Ti)  $>$   $D_{\text{Fe}}$  (in  $\alpha$ -Ti).<sup>38</sup> This trend remains valid even at some normalized reciprocal temperature  $T_m/T$ , where  $T_m$  is the melting temperature of Ti or Zr and is analogous to the analysis presented for amorphous alloys in the form of normalized plots of  $\ln(D)$  versus  $T_x/T$ . It is noted that the trend of impurity diffusivities in crystalline  $\alpha$ -Ti and  $\alpha$ -Zr, in fact, nearly resembles the observed trend of the corresponding diffusivities in the amorphous  $\text{Ti}_{60}\text{Ni}_{40}$  and  $\text{Zr}_{50}\text{Ni}_{50}$  alloys (cf. Fig. 5), and thus the difference in the diffusion rates in the two amorphous alloys seems to be related to the differences in the alloy matrices in the two cases. It appears that a replacement of Zr by Ti in a given type of M-M amorphous alloy may lead to a decrease in the impurity diffusion rates.

A word of caution would be advisable here in regard to drawing conclusions on the basis of a comparison of data on a normalized Arrhenius plot as shown in Fig. 5. The normalization parameter  $T_x$  is not a uniquely defined quantity because it is prone to variations by 20-80 K depending on the heating rates used for its measurement. Therefore, the  $T_x$  values at the same heating rate for the alloys considered in such a comparison must be used. However, normalized Arrhenius plots have been found to be quite useful when the comparison involves either the same diffusing species in several amorphous alloys or the different species in a given amorphous alloy system.<sup>5,7,39</sup>

## B. Validity of the size dependence

A size dependence of  $D$  according to which smaller atoms diffuse faster than bigger ones has previously been shown to hold in amorphous  $\text{Zr}_{61}\text{Ni}_{39}$  (Ref. 12) and  $\text{Zr}_{50}\text{Ni}_{50}$ .<sup>4</sup> It was suggested<sup>12</sup> that such size dependence is possibly a general feature of M-M-type amorphous alloys, but shows a number of exceptions in the case of M-Me-type amorphous alloys. Indeed, in a recent investigation on diffusion in the M-Me amorphous alloy  $\text{Fe}_{40}\text{Ni}_{40}\text{B}_{20}$ , it has been shown that the size dependence of  $D$  holds in this alloy for Be, Ni, Fe, Cu, P, Si, and Ti, but at the same time it does not hold for Au.<sup>5</sup> Exceptions from the rule were also observed in  $\text{Fe}_{82}\text{B}_{18}$ ,<sup>12</sup> where the

size dependence of  $D$  holds for Cu, Si, and Au, but fails for Al and Sb, and in  $\text{Pd}_{78}\text{Cu}_6\text{Si}_{16}$ ,<sup>6</sup> where the rule is observed for Pt, Au, Tl, Tb, and Bi, but does not hold for Ir, W, and Hg. It was argued<sup>5</sup> that the presence of metalloids and the resulting strong chemical effects between the matrix and the diffusing atoms may conceal an otherwise possible size dependence of  $D$  for certain diffusing species in these alloys.

With regard to Fig. 4 the validity of the size dependence of  $D$  for the impurity data obtained in the M-M-type amorphous  $\text{Ti}_{60}\text{Ni}_{40}$  is obvious when the different impurities are compared on the basis of their metallic radii for a coordination number of 12. It is seen that the small boron atoms (atomic size  $r_B = 0.098$  nm) diffuse about 2 orders of magnitude faster than the big silicon atoms ( $r_{\text{Si}} = 0.132$  nm) and the diffusivities of Be ( $r_{\text{Be}} = 0.112$ ) and Fe ( $r_{\text{Fe}} = 0.126$ ) have intermediate values following the trend  $D_B > D_{\text{Be}} > D_{\text{Fe}} > D_{\text{Si}}$ . This trend of the diffusivity values in amorphous  $\text{Ti}_{60}\text{Ni}_{40}$  is opposite to the trend of the atomic size of the diffusing impurity atoms, namely,  $r_B < r_{\text{Be}} < r_{\text{Fe}} < r_{\text{Si}}$ , thus indeed suggesting the size dependence of  $D$  in this alloy.<sup>22</sup> A plot of  $D$  versus the atomic radius  $r$  at 650 K, a temperature lying in the middle of the investigated temperature regime is shown in Fig. 6. It can be seen from Fig. 4 that the magnitude of the size dependence shown in Fig. 6 practically does not change over the entire temperature range 598–690 K investigated here.

The size dependence of  $D$  has been verified in several other M-M-type amorphous alloys beyond Zr-Ni and Ti-Ni, viz., in Zr-Fe,<sup>13</sup> Zr-Co,<sup>14</sup> and Ni-Nb.<sup>15,40</sup> Nevertheless, for M-M-type amorphous alloys this dependence, in all probability, is not general, because in  $\text{Zr}_{67}\text{Ni}_{33}$  (Ref. 41) and  $\text{Ni}_{60}\text{Nb}_{40}$  (Ref. 40) the impurity Pb is observed to diffuse faster than Au despite its larger atomic radius, and in  $\text{Zr}_{50}\text{Ni}_{50}$  the diffusivity of Ag is more than 1 order of magnitude higher than that of Au despite their atomic radii are practically equal.<sup>42</sup>

A correlation of the diffusion coefficient with the size of the diffusing atom can be interpreted qualitatively as being caused by different elastic distortions of the matrix during the thermally activated jump of the differently

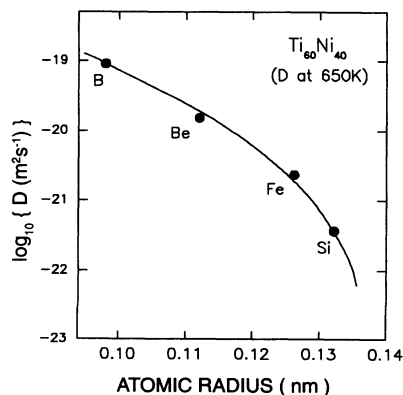


FIG. 6. The plot of the diffusion coefficient  $D$  of various diffusing species in the amorphous alloy  $\text{Ti}_{60}\text{Ni}_{40}$  at 650 K vs their atomic radii. The line was drawn visually.

sized atoms. Such an interpretation would imply an influence of the size of the effective activation energy  $Q$  as well. Recently for several M-M-type amorphous alloys a linear correlation of  $Q$  and the quantity  $kT_x(V_i/V_s)^{5/6}$  was proposed,<sup>12</sup> where the  $V_i$  and  $V_s$  are the molar volumes of the diffusing impurity and the smaller of the matrix atoms, respectively. This correlation does, in fact, represent the size dependence of the activation energy  $Q$  normalized to the crystallization temperature  $T_x$ . It is based on the assumption that  $T_x$  is proportional to the formation energy of a hole of the size of the smaller of the matrix atoms<sup>43,44</sup> and the relation has been simply scaled by the ratio of the molar volumes of the impurity and the matrix atom, i.e., by  $(V_i/V_s)^{5/6}$ , to represent the formation energy of a hole of size of the diffusing atom. It can be observed from Table IV and Fig. 7 that there is, within the experimental uncertainties, a trend of an increase in  $Q$  with an increase in the size of the diffusing impurity atom in amorphous  $\text{Ti}_{60}\text{Ni}_{40}$ . However, this trend is small compared to the FeNiB system. A similar trend of increasing  $Q$  with increase in the size of the diffusing atom is also noticed in other systematic investigations in both metal-metal-type  $\text{Zr}_{61}\text{Ni}_{39}$ ,  $\text{Zr}_{50}\text{Ni}_{50}$ ,<sup>4</sup> and metal-metalloid-type  $\text{Fe}_{40}\text{Ni}_{40}\text{B}_{20}$ ,<sup>5,29,30</sup> and  $\text{Pd}_{78}\text{Cu}_6\text{Si}_{16}$  (Ref. 6) amorphous alloys. The data reported in these investigations are collected in Table V.

The atomic size effect on diffusion is only one of several factors affecting the diffusion rate. Other factors are the structure of the matrix and the electronic configuration of the impurity and the solvent species. A clear size dependence can be expected only if chemically and

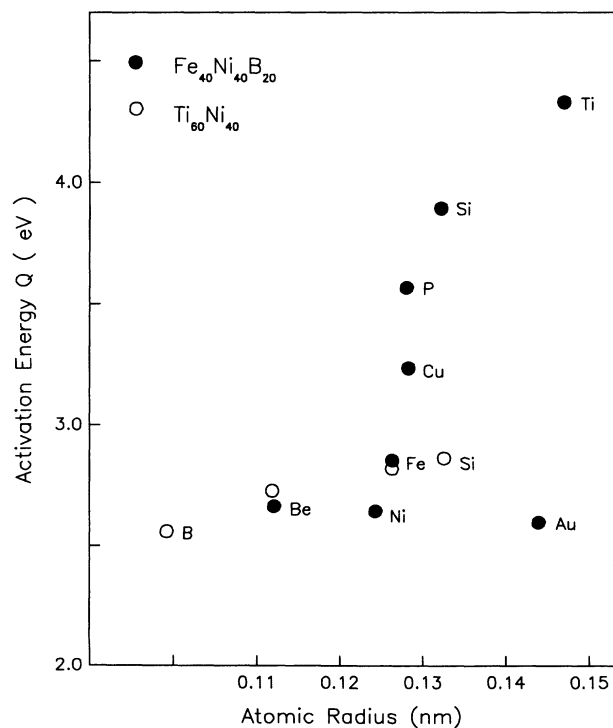


FIG. 7. The plot of the activation energy  $Q$  of various diffusing species in the amorphous alloys  $\text{Ti}_{60}\text{Ni}_{40}$  (cf. Table IV) and  $\text{Fe}_{40}\text{Ni}_{40}\text{B}_{20}$  (Ref. 5) vs their atomic radii.

TABLE V. Size dependence of the activation energy for different amorphous alloys.

Alloy system	Impurity	Atomic radius (nm)	$Q$ (eV)
Zr <sub>61</sub> Ni <sub>39</sub> Ref. 12	Cu	0.128	1.33
	Au	0.144	1.66
	Al	0.143	1.68
	Sb	0.159	2.07
Zr <sub>50</sub> Ni <sub>50</sub> Ref. 4	Ni	0.124	1.45
	Co	0.125	1.40
	Cu	0.128	1.57
	Fe	0.126	1.64
	Au	0.144	1.77
Pd <sub>78</sub> Cu <sub>16</sub> Si <sub>6</sub> Ref. 6	Pt	0.138	1.39
	Au	0.144	2.10
	Tl	0.171	2.70
	Hg	0.157	2.79
	Pb	0.175	2.98
	W	0.139	3.19
	Bi	0.170	3.69
	Ir	0.136	3.99

structurally similar systems are compared. It seems that the M-M-type amorphous alloys are systems for which chemical and structural effects are less important than for M-Me-type amorphous alloys. Finally we should emphasize that in case of a clear dependence of the diffusivity and of the effective activation energy on the size of the diffusing impurity, a preferential single jump mechanism of diffusion is indicated since the specific impurity and not the matrix atoms surrounding it obviously determine the diffusion jump in this case.

### C. Comparison of the diffusion behavior in amorphous alloys and crystals

The observation of linear Arrhenius plots representing the temperature dependence of  $D$  is suggestive of some specific mechanism of diffusion in these alloys. The absence of translational periodicity in amorphous alloys will lead to the assumption that the local atomic structure is different at each point in these materials. As a result the potential barrier for atomic migration should be non-periodic and of different heights. Under these conditions the measured values of  $D_0$  and  $Q$  would represent average values over many different diffusion jumps. However, on the basis of observed straight Arrhenius plots for diffusion it was suggested<sup>45-47</sup> that the distribution of activation barrier heights to individual diffusion jumps is fairly narrow in amorphous alloys.

On the basis of this observation diffusion in amorphous alloys can be characterized by the two experimental diffusion parameters, the prefactor  $D_0$  and the activation energy  $Q$ , which are determined by the diffusion mechanism. It is expected that varying diffusion mechanisms between crystalline and amorphous alloys will show up in a different behavior of these parameters. An empirical correlation between the prefactors and the activation energies of reaction rates of closely related chemical reac-

tions has been frequently observed and is known as the isokinetic relation or compensation effect.<sup>48,49</sup> For diffusion rates this relationship leads to

$$\ln D_0 = \ln A + Q/B, \quad (3)$$

which is expected to be fulfilled with specific parameters  $A$  and  $B$  for a whole set of diffusion coefficients if they are based on a common diffusion mechanism. However, the equivalence of two diffusion mechanisms cannot necessarily be concluded from a near coincidence in the parameters  $A$  and  $B$ .

Figure 8 shows a plot of  $\ln D_0$  versus  $Q$  for the diffusion data reported in systematic studies of several metal-metal-type Zr- and Ti-based amorphous alloys. In spite of the relatively large scatter the data are obviously correlated according to Eq. (3) with the values of the parameters  $A$  and  $B$  as  $9.8 \times 10^{-21} \text{ m}^2 \text{ s}^{-1}$  and 0.053 eV, respectively. These values are determined mainly by the data obtained on Zr-based amorphous alloys which cover the large range of more than 20 orders of magnitude in  $D_0$ . The parameters  $A$  and  $B$  are the same within experimental uncertainty as were reported for several amorphous alloys<sup>12,50</sup> and for Fe<sub>40</sub>Ni<sub>40</sub>B<sub>20</sub> and Pd<sub>78</sub>Cu<sub>16</sub>Si<sub>6</sub> in a recent investigation.<sup>5</sup> In order to see any distinct difference between the amorphous Zr- and Ti-based alloys and the crystalline  $\alpha$ -Zr and  $\alpha$ -Ti, the data reported for crystalline  $\alpha$ -Zr and  $\alpha$ -Ti (Refs. 36 and 37) have also been plotted in Fig. 8. Only the data reported in high-purity single crystals have been considered in this plot. The main reason for doing so stems from the fact that the presence of impurities in these materials are known to have a drastic effect on the diffusion behavior of a given species and thus the data obtained only in high-purity

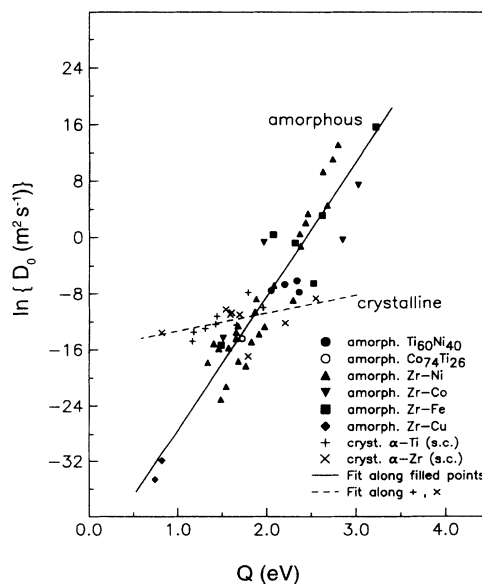


FIG. 8. The plot of  $\ln D_0$  vs  $Q$ . Each symbol represents the data for self- or impurity diffusion in a given matrix. The data for different matrices have been taken from Ti<sub>60</sub>Ni<sub>40</sub> (Table IV); Ti-Co (Ref. 23), Zr-Ni, Zr-Co, Zr-Fe, Zr-Cu (Ref. 10), and  $\alpha$ -Ti,  $\alpha$ -Zr (Ref. 38).

single crystals can be regarded to be least influenced by such effects.<sup>51</sup> Though there are not many data points available in crystalline  $\alpha$ -Zr and  $\alpha$ -Ti,<sup>42</sup> a trend which is quite different from that observed for amorphous alloys arises from Fig. 8 leading to  $A = 1.4 \times 10^{-7} \text{ m}^2/\text{s}$  and  $B = 0.35 \text{ eV}$ . A similar comparison has been performed for the data obtained in amorphous  $\text{Fe}_{40}\text{Ni}_{40}\text{B}_{20}$  and  $\text{Pd}_{78}\text{Cu}_{16}\text{Si}_6$  and the corresponding crystalline alloy constituents Fe, Ni, Pd, and Cu (Ref. 5) yielding also distinctly different trends in the amorphous and the crystalline cases. The parameters  $A$  and  $B$  are summarized in Table VI. This table also includes the values obtained for hydrogen diffusion in amorphous alloys which are quite different from those for the diffusion of all other diffusing atoms.<sup>12</sup> The other noteworthy feature from Table VI pertains to the fact that the values of  $A$  and  $B$  are practically the same in a given class of materials, i.e., either amorphous or crystalline, thus suggesting that the atomic migration process in the materials of a given class (either in M-M/M-Me-type amorphous alloys, or in crystalline materials) must be similar. However, the different values obtained for  $A$  and  $B$  for the amorphous and crystalline materials are indicative of different diffusion mechanism in the two cases.

With regard to the compensation effect, the parameters  $A$  and  $B$  are the coordinates of a common intersection point of the family of diffusion coefficients in the Arrhenius plot.<sup>49</sup> The mean temperature  $T_{\text{iso}} = B/k_B$  of this intersection derived for all the values of the Zr- and Ti-based amorphous alloys shown in Fig. 8 amounts to less than 700 K. By inspection of the individual Arrhenius plots of the  $\text{Ti}_{60}\text{Ni}_{40}$  amorphous alloy in Fig. 4 a common intersection point of  $T_{\text{iso}}$  of about 2000 K is estimated, significantly different from the mean value even with regard to the uncertainties given in Table IV for the individual diffusion parameters. Although the importance of this difference is not clear, it does not invalidate the above general statement that different diffusion mechanisms are operating in amorphous and crystalline materials.

If diffusion in amorphous alloys can be described by jump processes like the diffusion in crystals then the pa-

rameters  $A$  and  $B$  are identified as<sup>52</sup>

$$A = a^2 g f \nu_0, \quad (4)$$

$$B = k_B Q / \Delta S. \quad (5)$$

Here  $a$  is the effective jump distance,  $g$  the geometric factor,  $f$  the correlation factor,  $\nu_0$  the jump attempt frequency, and  $\Delta S$  represents the change in the activation entropy during the jump process. In the framework of this crystalline analogy to diffusion in amorphous materials, the large difference of more than 10 orders of magnitude between the values of  $A$  for the amorphous and the crystalline cases must result from the significantly different values of the various constituent factors in Eq. (4) in the two cases. It may be possible to account to some extent for the low value of  $A$  in the case of amorphous alloys in terms of the low values of all these factors, namely,  $\nu_0$ ,  $a$ , and  $f$ , which in crystals take on values of approximately  $10^{13} \text{ s}^{-1}$ , one lattice spacing, and near unity, respectively.

There are experimental and theoretical indications that the attempt jump frequency  $\nu_0$  and the mean jump distance  $a$  are smaller in amorphous than in crystalline materials. From a study of internal friction of the amorphous  $\text{Pd}_{77.5}\text{Cu}_6\text{Si}_{16.5}$  alloy<sup>53</sup> it was concluded that a certain internal friction maximum which appeared around 640 K, i.e., below the crystallization temperature, was related to the mobility of a cluster of about 100 atoms. The relaxation frequency was observed to be thermally activated with an attempt frequency of  $\nu_0 \approx 5 \times 10^9 \text{ s}^{-1}$ , much smaller than the generally assumed value of  $10^{13} \text{ s}^{-1}$  in crystalline materials. This observation fits to recent calculations<sup>54</sup> which showed that localized low-frequency vibrational modes exist in soft-potential model glasses, and that up to 100 atoms participate in the soft-mode performing jump distances of a few percent of the mean atomic distance. The evaluation of the correlation factor  $f$  for such a complex diffusion mechanism, which is not so straightforward as known in crystalline cases,<sup>24</sup> is really difficult.<sup>55</sup> For a highly correlated diffusion process as would be the case for a mechanism involving several atoms, the  $f$  is expected to attain a value much smaller than unity.<sup>56</sup> However, unless the correlation fac-

TABLE VI. The values of the parameters  $A$  and  $B$  [cf. Eq. (3) of the text] in different systems.

System	$A$ ( $\text{m}^2 \text{ s}^{-1}$ )	$B$ (eV)	Ref.
Amorph. Zr- and Ti-based alloys	$9.8 \times 10^{-21 \pm 1.5}$	$0.053 \pm 0.005$	This work
Single-cryst. $\alpha$ -Ti and $\alpha$ -Zr	$1.4 \times 10^{-7}$	0.384	This work
Amorph. FeNiB and PdCuSi	$9.5 \times 10^{-21}$	0.054	5
Cryst. Fe, Ni, Cu, and Pd	$2.8 \times 10^{-7}$	0.412	5
M-Me- and M-M-type amorph. alloys	$8.5 \times 10^{-20}$	0.054	12
Hydrogen in amorph. alloys	$8.9 \times 10^{-11}$	0.038	12

tor becomes extremely small the above evidences for a cooperative jump mechanism are not sufficient to explain quantitatively the huge difference of the parameter  $A$  derived for amorphous and the crystalline material by using an expression like Eq. (4).

A linear relation between the activation energy  $Q$  and the entropy change  $\Delta S$  as given by Eq. (5) has been derived earlier for interstitial diffusion in bcc metals, e.g., for the diffusion of carbon in  $\alpha$ -Fe, by using thermodynamic considerations.<sup>57,58</sup> As a result of these considerations, the parameter  $B$  was related to the temperature dependence of the elastic modulus, and  $B \approx k_B T_m / 0.35$  was predicted in accordance with experimental observation. It was shown that a similar relation holds for impurity diffusion in fcc crystals. The entropy change  $\Delta S$ , according to Eq. (5), is then derived to be  $(1-5)k_B$  depending on the actual activation energy and melting temperature of the crystal. In amorphous alloys the parameter  $B$  is about 1 order of magnitude smaller than in crystals (cf. Table VI) which implies an entropy change  $\Delta S$  for diffusion in these materials of  $(20-40)k_B$ . This large value suggests cooperative motion of a larger number of atoms in a qualitative accord with the discussion on the parameter  $A$  in the previous paragraph. Therefore, considering the above interpretation of the values of the parameters  $A$  and  $B$  together, the observed low value of  $A$  and a significantly large value of  $\Delta S$  in our analysis of diffusion data tend to suggest that the diffusion mechanism in amorphous alloys possibly involves a collective motion by a group of atoms rather than a single atom jump as in crystals. However, a quantitative description cannot be achieved by the usually applied schemes of interpretation. In this context it is noteworthy that the values of  $A$  and  $B$  obtained for hydrogen diffusion in amorphous alloys,<sup>12</sup> when interpreted as given above, suggest that hydrogen diffuses by an interstitial process.

In the following, other experimental results relevant for an understanding of the diffusion mechanism in amorphous alloys are discussed. Impurities in substitutional metal crystals generally diffuse via vacancies in thermal equilibrium, i.e., via localized point defects, which can be identified by the pressure dependence and the isotope effect of the diffusion coefficient. The possible existence of vacancylike defects in thermal equilibrium in relaxed amorphous  $\text{Co}_{76.7}\text{Fe}_2\text{Nb}_{14.3}\text{B}_7$  was investigated recently by performing for the diffusing cobalt atoms both pressure dependence and isotope effect measurements.<sup>59</sup> A vanishingly small pressure dependence and a very weak isotope effect of  $E=0.1$  were found which led to the conclusion that cobalt diffusion in this alloy does not occur via a vacancylike defect but by a cooperative mechanism involving some ten atoms. Further measurements of isotope effect in the same material<sup>60</sup> showed that in the as-quenched state vacancylike defects are present which annealed during the thermal relaxation of the material. This result was interpreted as a transition from a preferential single-atom jump mechanism operating in the as-quenched state, to a highly cooperative diffusion mechanism in the structurally relaxed state of the metallic glass. However, the results of these measurements are in con-

trast to similar measurements of the pressure dependence of Co diffusion in amorphous Zr-Ni alloys,<sup>61</sup> where an activation volume of  $\sim(8-20) \times 10^{-30} \text{ m}^3$  was estimated which is slightly larger than one atomic volume. A similar value was also derived from an analysis of the crystallization kinetics of amorphous  $(\text{FeNi})_8(\text{PB})_2$ .<sup>62</sup>

The contrasting results of activation volume obtained by pressure effect measurements in amorphous  $\text{Co}_{76.7}\text{Fe}_2\text{Nb}_{14.3}\text{B}_7$  (Ref. 59) and  $(\text{FeNi})_8(\text{PB})_2$  (Ref. 62) alloys, which are both of M-Me type, were rationalized<sup>63</sup> within the model of free volume by assuming two possible types of activation volume: a larger one existing at high temperatures near the glass transition ( $\Delta V_{\text{equilib}}$ ) and a smaller one existing at lower temperatures ( $\Delta V_{\text{iso-config}}$ ). This interpretation does not hold, however, if the high activation volume observed in the relaxed M-M-type Zr-Ni alloy<sup>61</sup> at the low temperature of 573 K is considered. It is yet an open question, whether or not these discrepancies result from possible structural differences between the different amorphous alloys.

The interpretation of the data reported in this paper brings out two points which are not reconcilable. On the one hand, it has been shown that the diffusivity and the activation energy of diffusion depend on the size of the diffusing impurity (cf. Figs. 6 and 7, and Table V). This observation would indicate a preferential single-jump mechanism of the impurity. On the other hand, the observed isokinetic relation (cf. Fig. 8) suggests that a fundamentally different diffusion mechanism is operating in the amorphous alloys as compared to that in crystalline material. An interpretation of this effect in terms of parameters like attempt frequency, jump distance, correlation factor, and entropy change during the jump would suggest that a cooperative jump mechanism is operating in amorphous alloys. The available pressure effect measurements are not helpful to resolving the conflicting interpretations as they show mutually inconsistent results. This shows clearly that the pin-pointing of the actual diffusion mechanism in amorphous alloys is still debatable.

## V. CONCLUSIONS

The measurement of tracer diffusion coefficients  $D$  of several impurity atoms in amorphous  $\text{Ti}_{60}\text{Ni}_{40}$  in the temperature range 598–690 K by SIMS indicated the following.

(i) B atoms with the smallest size had the highest diffusion rates followed by those of Be, Fe, and Si. This trend of the diffusivities is opposite to the trend of the atomic radii of the diffusing species, thus suggesting the size dependence of  $D$  in this amorphous alloy.

(ii) The measured diffusion coefficients can be described by the Arrhenius relation  $D = D_0 \exp(-Q/k_B T)$  in the temperature range between 598 and 690 K, yielding the activation energy  $Q$  as  $(2.05 \pm 0.14)$ ,  $(2.20 \pm 0.15)$ ,  $(2.33 \pm 0.14)$ , and  $(2.35 \pm 0.15)$  eV for the diffusion of B, Be, Fe, and Si, respectively. These values are indicative of a trend of the increasing activation energy with the increase in the size of the diffusing impurity atom and thus

of a size dependence of the activation energy.

(iii) A comparison of the diffusion data in amorphous  $\text{Ti}_{60}\text{Ni}_{40}$  and those reported in Zr-based amorphous alloys with the available data in crystalline  $\alpha$ -Ti and  $\alpha$ -Zr suggests a trend according to which the diffusivity is generally smaller in Ti-based alloys than in Zr-based alloys.

(iv) A comparison of the diffusion parameters  $D_0$  and  $Q$  in the amorphous  $\text{Ti}_{60}\text{Ni}_{40}$  and other amorphous alloys with those available in the corresponding crystalline constituents suggests that the atom transport mechanism in amorphous alloys is different from that operating in crystals.

#### ACKNOWLEDGMENTS

The authors would like to thank Professor H. Wollenberger for his constant encouragement during the course of this work and for his valuable comments and suggestions on the manuscript. Financial support to one of us (S.K.S.) from the Alexander von Humboldt-Stiftung, Bonn (Germany) is gratefully acknowledged. Thanks are due to D. Köpnick and I. Dencks for their assistance in the specimen preparation and to Dr. H. R. Hilzinger of Vakuumschmelze, Hanau for providing us with the  $\text{Ti}_{60}\text{Ni}_{40}$  amorphous ribbon.

\*Present address: Condensed Matter Physics Lab., Department of Physics, University of Rajasthan, Jaipur 302 004, India.

- <sup>1</sup>R. W. Cahn, in *Physical Metallurgy*, edited by R. W. Cahn and P. Haasen (Elsevier, Amsterdam, 1983), p. 1779.
- <sup>2</sup>W. L. Johnson, *Prog. Mater. Sci.* **30**, 81 (1986).
- <sup>3</sup>J. Horvath, J. Ott, K. Pfahler, and W. Ulfert, *Mater. Sci. Eng.* **97**, 409 (1988).
- <sup>4</sup>H. Hahn, R. S. Averbach, and H.-M. Shyu, *J. Less Common Met.* **140**, 345 (1988).
- <sup>5</sup>S. K. Sharma, M.-P. Macht, and V. Naundorf, *Acta Metall. Mater.* **40**, 2439 (1992).
- <sup>6</sup>J. Bottiger, K. Dyrbye, K. Pampus, B. Torp, and P. H. Wiene, *Phys. Rev. B* **37**, 9951 (1988).
- <sup>7</sup>B. Cantor and R. W. Cahn, in *Amorphous Metallic Alloys*, edited by F. E. Luborsky (Butterworths, London, 1983), p. 487.
- <sup>8</sup>H. Mehrer and W. Dörner, *Defect Diffusion Forum* **66-69**, 189 (1989).
- <sup>9</sup>R. W. Cahn, in *Proceedings of the 2nd International Workshop on Non-Crystalline Solids*, San Sebastian (World Scientific, Singapore, to be published).
- <sup>10</sup>J. Horvath, in *Diffusion in Solid Metals and Alloys*, edited by H. Mehrer, Landolt-Börnstein, New Series, Group 3, Vol. 26 (Springer, Berlin, 1990), p. 437.
- <sup>11</sup>S. K. Sharma, S. Banerjee, Kuldeep, and A. K. Jain, *Appl. Phys. A* **45**, 217 (1988).
- <sup>12</sup>S. K. Sharma, S. Banerjee, Kuldeep, and A. K. Jain, *J. Mater. Res.* **4**, 603 (1989).
- <sup>13</sup>J. Horvath, K. Pfahler, W. Ulfert, W. Frank, and H. Kronmüller, *Mater. Sci. Forum* **15-18**, 523 (1987).
- <sup>14</sup>W. Dörner and H. Mehrer, *Phys. Rev. B* **44**, 101 (1991).
- <sup>15</sup>M. M. Kijek, D. W. Palmer, and B. Cantor, *Acta Metall.* **34**, 1455 (1986).
- <sup>16</sup>K. H. J. Buschow, *J. Appl. Phys.* **56**, 304 (1984).
- <sup>17</sup>D. E. Polk, A. Calka, and B. C. Giessen, *Acta Metall.* **26**, 1097 (1978).
- <sup>18</sup>L. E. Tanner and R. Ray, *Scr. Metall.* **11**, 783 (1977).
- <sup>19</sup>K. H. J. Buschow, *J. Phys. F* **13**, 563 (1983).
- <sup>20</sup>H. Ruppertsberg, C. Görlitz, and B. Heck, *J. Phys. F* **14**, 309 (1984).
- <sup>21</sup>S. K. Sharma, M.-P. Macht, and V. Naundorf, *Scr. Metall.* **25**, 755 (1991).
- <sup>22</sup>S. K. Sharma, M.-P. Macht, and V. Naundorf, *Phys. Rev. B* **46**, 3147 (1992).
- <sup>23</sup>F. La Via, K. T. F. Janssen, and A. H. Reader, *Appl. Phys. Lett.* **60**, 701 (1992).
- <sup>24</sup>P. G. Shewmon, in *Diffusion in Solids* (McGraw-Hill, New York, 1963), p. 62.
- <sup>25</sup>M.-P. Macht and V. Naundorf, *J. Appl. Phys.* **53**, 7551 (1982).
- <sup>26</sup>M.-P. Macht, R. Willecke, and V. Naundorf, *Nucl. Instrum. Methods B* **43**, 507 (1989).
- <sup>27</sup>A. J. Janicki and P. J. Grundi, *J. Phys. D* **19**, L49 (1986).
- <sup>28</sup>M. A. Hollanders and B. J. Thijssse, *J. Non-Cryst. Solids* **117/118**, 696 (1990).
- <sup>29</sup>R. W. Cahn, J. E. Evetts, J. Patterson, R. E. Somekh, and C. K. Jackson, *J. Mater. Sci.* **15**, 702 (1980).
- <sup>30</sup>J. Horvath and H. Mehrer, *Cryst. Lattice Defects Amorph. Mater.* **13**, 1 (1986).
- <sup>31</sup>S. K. Sharma, P. Mukhopadhyay, Kuldeep, and A. K. Jain, *J. Non-Cryst. Solids* **94**, 294 (1987).
- <sup>32</sup>Y. Waseda, *Prog. Mater. Sci.* **26**, 1 (1981).
- <sup>33</sup>J. Wang, in *Glassy Metals I*, edited by H.-J. Güntherodt and H. Beck (Springer, Berlin, 1981), p. 74.
- <sup>34</sup>G. S. Cargill, III, *Solid State Phys.* **30**, 227 (1975).
- <sup>35</sup>K. H. J. Buschow, in *Proceedings of the 5th International Conference on Rapidly Quenched Metals*, edited by S. Steeb and H. Warlimont (North-Holland, Amsterdam, 1985), Vol. I, p. 163.
- <sup>36</sup>M. Nakajima and M. Koiwa, *Defect Diffusion Forum* **66-68**, 395 (1989).
- <sup>37</sup>G. M. Hood, *J. Nucl. Mater.* **139**, 179 (1986).
- <sup>38</sup>A. D. Le Claire and G. Neumann, *Diffusion in Solid Metals and Alloys* (Ref. 10), p. 85.
- <sup>39</sup>S. K. Sharma, S. Banerjee, Kuldeep, and A. K. Jain, *Appl. Phys. A* **50**, 365 (1990).
- <sup>40</sup>D. Akhtar and R. D. Misra, *Scr. Met.* **19**, 603 (1985).
- <sup>41</sup>D. Akhtar, B. Cantor, and R. W. Cahn, *Scr. Met.* **16**, 417 (1982).
- <sup>42</sup>E. C. Stelter and D. Lazarus, *Phys. Rev. B* **36**, 9545 (1987).
- <sup>43</sup>K. H. J. Buschow and N. M. Beekmans, *Solid State Commun.* **35**, 233 (1980).
- <sup>44</sup>A. W. Weeber, *J. Phys. F* **17**, 809 (1987).
- <sup>45</sup>A. K. Tyagi, M.-P. Macht, and V. Naundorf, *Acta Metall. Mater.* **39**, 609 (1991).
- <sup>46</sup>B. Cantor, in *Amorphous Metals and Semiconductors*, edited by P. Haasen and R. I. Jaffee (Pergamon, Oxford, 1986), p. 108.
- <sup>47</sup>Y. Limoge, *Defect Diffusion Forum* **83**, 145 (1992).
- <sup>48</sup>S. Wach, *Diffusion Defect Monograph* (Trans. Tech. Switzerland, 1983), Series No. 7, p. 454.
- <sup>49</sup>W. Linert, *Chem. Soc. Rev.* **18**, 477 (1989).
- <sup>50</sup>H. Kronmüller and W. Frank, *Radiat. Eff. Defects Solids* **108**, 81 (1989).
- <sup>51</sup>G. M. Hood, *J. Nucl. Mater.* **159**, 149 (1988).
- <sup>52</sup>A. D. LeClaire, in *Progress in Metal Physics*, edited by B. Chalmers (Pergamon, Oxford, 1949), Vol. 1, p. 306.
- <sup>53</sup>L. X.-Guang, Z. Yuheng, and H. Yizhen, *J. Phys.: Condens.*

- Matter **2**, 809 (1990).
- <sup>54</sup>U. Buchenau, Yu. M. Galperin, V. L. Gurevich, and H. R. Schober, Phys. Rev. B **43**, 5039 (1991).
- <sup>55</sup>M. Koiwa, M. Arita, and S. Ishioka, Defect Diffusion Forum **66-69**, 65 (1989).
- <sup>56</sup>H. J. de Bruin and G. E. Murch, Philos. Mag. **27**, 1475 (1973).
- <sup>57</sup>C. Zener, *Imperfections in Nearly Perfect Crystals* (Wiley, New York, 1952).
- <sup>58</sup>C. P. Flynn, *Point Defects and Diffusion* (Clarendon, Oxford, 1972), p. 335.
- <sup>59</sup>F. Faupel, P. W. Hüppe, and K. Rätzke, Phys. Rev. Lett. **65**, 1219 (1990).
- <sup>60</sup>K. Rätzke, P. W. Hüppe, and F. Faupel, Phys. Rev. Lett. **68**, 2347 (1992).
- <sup>61</sup>H. J. Höfler, R. S. Averback, G. Rummel, and H. Mehrer, Philos. Mag. Lett. **66**, 301 (1992).
- <sup>62</sup>Y. Limoge, Acta Metall. Mater. **38**, 1733 (1990).
- <sup>63</sup>F. Spaepen and D. Turnbull, Scr. Metall. **25**, 1563 (1991).